ResearchGate

See discussions, stats, and author profiles for this publication at: https://www.researchgate.net/publication/275217012

Mussel-Inspired Hybrid Coatings that Transform Membrane Hydrophobicity into High Hydrophilicity and Underwater Superoleophobicity for Oil-in-Water Emulsion Separation

ARTICLE *in* ACS APPLIED MATERIALS & INTERFACES · APRIL 2015

Impact Factor: 6.72 · DOI: 10.1021/acsami.5b00894 · Source: PubMed

CITATIONS
9

READS
41

5 AUTHORS, INCLUDING:

Zhenxing Wang
Harbin Institute of Technology
12 PUBLICATIONS **129** CITATIONS
SEE PROFILE

Cher Hon Lau
The Commonwealth Scientific and Industrial …
24 PUBLICATIONS **360** CITATIONS
SEE PROFILE

Lu Shao
Harbin Institute of Technology
79 PUBLICATIONS **1,400** CITATIONS
SEE PROFILE

Available from: Zhenxing Wang
Retrieved on: 04 February 2016

ACS APPLIED MATERIALS & INTERFACES

Research Article

www.acsami.org

Mussel-Inspired Hybrid Coatings that Transform Membrane Hydrophobicity into High Hydrophilicity and Underwater Superoleophobicity for Oil-in-Water Emulsion Separation

Zhenxing Wang,[†] Xu Jiang,[†] Xiquan Cheng,[†,‡] Cher Hon Lau,*[,‡] and Lu Shao*[,†]

[†]State Key Laboratory of Urban Water Resource and Environment (SKLUWRE), School of Chemical Engineering and Technology, Harbin Institute of Technology, Harbin 150001, P.R. China

[‡]Manufacturing Flagship, CSIRO, Private Bag 10, Clayton, Victoria 3168, Australia

Supporting Information

ABSTRACT: We first report here mussel-inspired, hybrid coatings formed in a facile manner via simultaneous polymerization of mussel-inspired dopamine and hydrolysis of commercial tetraethoxysilane in a single-step process. The hybrid coatings can firmly adhered on hydrophobic polyvinylidene fluoride (PVDF) substrate, and the hydrophilicity of the coating can be tuned by adjusting silane concentration. The reason for the changed hydrophilicity of the coating is disclosed by a series of characterization, and was applied to rationally design optimized hybrid coatings that transform commercial PVDF microfiltration (MF) membrane hydrophobicity into high hydrophilicity with excellent water permeability and underwater superoleophobicity for oil-in-water emulsion separation. The PVDF MF membrane decorated with optimized coatings has ultrahigh water flux (8606 L m^{-2} h^{-1} only under 0.9 bar, which is 34 times higher than that of pristine membrane), highly efficient oil-in-water emulsion separation ability at atmospheric pressure (filtrate flux of 140 L m^{-2} h^{-1}) and excellent antifouling performance. More importantly, these membranes are extremely stable as underwater superoleophobicity are maintained, even after rigorous washings or cryogenic bending, disclosing outstanding stability. The simplicity and versatility of this novel mussel-inspired one-step strategy may bridge the material-induced technology gap between academia and industry, which makes it promising for eco-friendly applications.

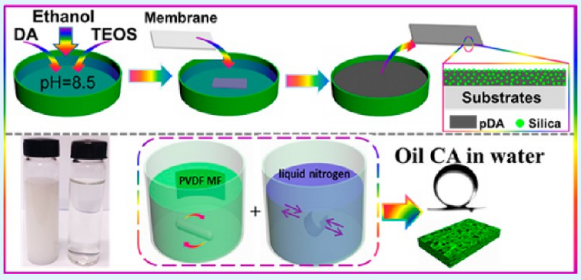

KEYWORDS: *hybrid coating, high hydrophilicity, underwater superoleophobicity, oil-in-water emulsion separation, long-term stability*

1. INTRODUCTION

Oily emulsion separations are crucial for tackling environmental and economic problems brought by the ever-increasing oily wastewater discharges from industries and oil spills.[1−5] Thus, desirable materials that can efficiently separate oil from water are urgently needed.[6] Porous filters like porous polymer membranes, and inorganic/metal meshes with special wettability have attracted extensive interest for their excellent separation selectivity, efficiency and recyclability in oil/water separation.[7−11] Such filters are typically categorized into "oil-removing" and "water-removing" filter materials.[12] "Water-removing" filter materials are usually highly hydrophilic or even superhydrophilic, and underwater superoleophobic with low oil adhesion, endowing such (membrane or mesh) materials with favorable antifouling properties, performance longevity, and recyclability of both oil and filter materials.[12−16] More importantly, "water-removing" filters can also be deployed for gravity driven separation processes that consumes less energy, which is more attractive for industrial applications.[13,17−19] Therefore, it is of great significance to develop "water-removing" filter materials for eco-friendly separations of oil from water.

For metal or inorganic mesh, dip-coating method is a facile and effective approach, and many kinds of "water-removing" filter materials had been fabricated by constructing highly hydrophilic coatings on metal mesh or inorganic filter through dip-coating approach.[7,13] Compared with metal or inorganic mesh, porous polymer membranes possess many exceptional advantages such as low cost, good processability and high flexibility, differentiating them from their inorganic or metallic counterparts.[20−22] However, for porous hydrophobic polymer membranes, most dip-coating methods are ineffective because of the poor adhesion or interactions between the coating layers and hydrophobic polymer membrane surface;[23,24] thus, special and complicated methods are usually needed to transform them into "water-removing" filter materials, diminishing the advantages of porous polymer membrane. Therefore, endowing hydrophobic polymer membranes with stable and high hydrophilicity and underwater superoleophobicity with low oil adhesion via a facile method are particularly promising for oily wastewater treatment.[25]

Received: January 29, 2015
Accepted: April 20, 2015
Published: April 20, 2015

ACS Publications © 2015 American Chemical Society

DOI: 10.1021/acsami.5b00894
ACS Appl. Mater. Interfaces 2015, 7, 9534−9545

Scheme 1. Illustration for the Immobilization of Hybrid Coatings on PVDF Substrates

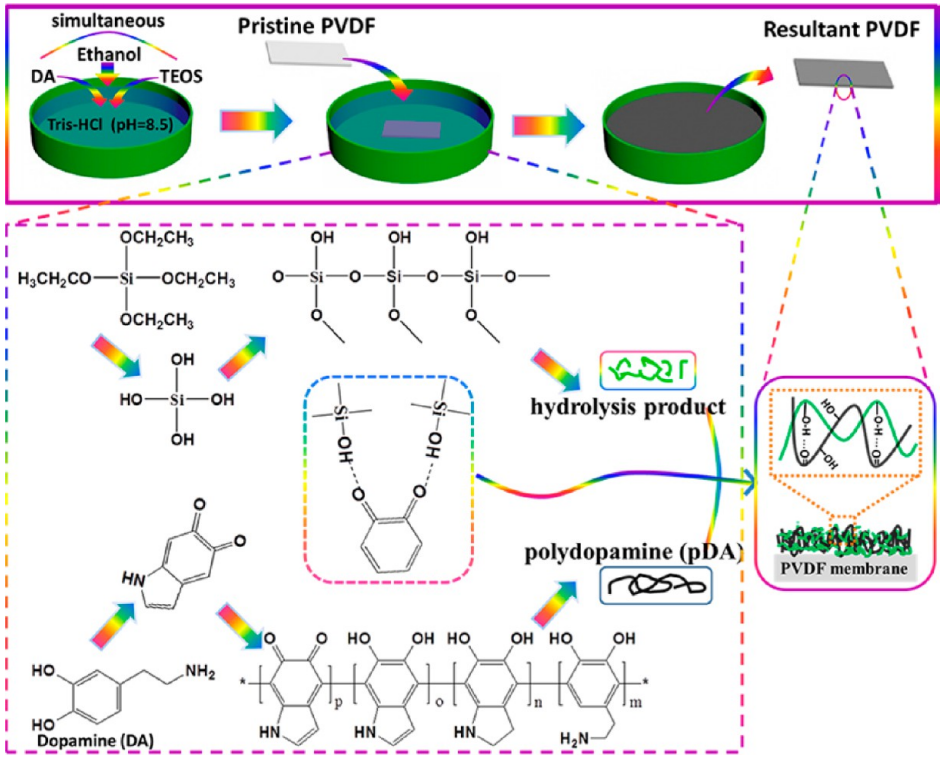

Recently, mussel-inspired coating approach with dopamine (DA) has been widely utilized to modify various materials for its stability, simplicity, and versatility,[26−30] although the exact polymerization and interaction mechanism of the adhesive pDA layer was kept unknown so far.[31−34] Different from traditional coating strategies, the mussel-inspired coating protocol involves an oxidative polymerization process,[33,35,36] yielding polydopamine (pDA) coatings that adhere to virtually all types of substrates with high binding strength.[26,37] However, it remains difficult to obtain "water-removing" porous filter for oil/water separation by pure pDA coating because of the inherent and limited hydrophilicity of pDA.[38,39] Subsequent modifications on the pDA layer that are usually time-consuming and complicated have to be adopted to further improve hydrophilicity of substrates.[20,40] Therefore, mussel-inspired one-step methods have been attracting more attention because rof their higher efficiency compared to common two-step methods. In mussel-inspired one-step methods, molecules with special functional groups dissolved with dopamine can be immobilized onto various surfaces during the pDA formation via hydrogen bonding, entanglement of molecular chain, or chemical reaction.[39,41,42] These molecules are usually limited to polar organic molecules, polymer with ultrahigh molecular weight, or molecules with amine/thiol groups,[38,39,42] and most of them are expensive and difficult to obtain such as dextran with ultrahigh molecular weight or zwitterionic peptides, restricting the extensive application. We found that some molecules such as tetraethoxysilane (TEOS) have been ignored because of their absence of hydroxyl group, amine/thiol groups, or ultrahigh molecular weight. Note that TEOS can gradually hydrolyze and condense under an alkaline environment, and form silica with abundant hydroxyl group. These hydrophilic nanoparticles may be fixed by pDA during the formation of pDA layer on substrates and thus form hybrid and highly hydrophilic coatings with favorable stability. Moreover, TEOS is inexpensive and easily obtained. All these make TEOS a potential and promising candidate for mussel-inspired one-step method.

Herein, we utilized commercially available and low-cost TEOS in this mussel-inspired one-step method (Scheme 1) to form hybrid coatings that can be firmly deposited on hydrophobic PVDF substrate. The wettability of the hybrid coatings can be well tuned by adjusting TEOS content. The reason for the improved hydrophilicity of the coatings are disclosed by a serials of characterization, and was applied to rationally design optimized hybrid coatings that transform membrane hydrophobicity into high hydrophilicity and underwater superoleophobicity with low oil adhesion for oil-in-water separation. The oily emulsion separation performance and antifouling property of the modified PVDF microfiltration membrane has been evaluated. Furthermore, the stability of the obtained PVDF microfiltration membrane is examined by long-term water washing and even being bent repeatedly in cryogenic conditions.

2. EXPERIMENTAL SECTION

2.1. Materials. PVDF powder was obtained from Inner Mongolia 3FWanHao Fluorine Chemical Co. Ltd. The commercial PVDF microfiltration membranes are purchased from Membrane Solution (USA). Dopamine hydrochloride and tris (hydroxymethyl)-aminomethane (Tris) were provided by Sigma-Aldrich (USA) and Aladdin (China), respectively. Carbon fibers are obtained from Toray Industries, Inc. Tetraethoxysilane (TEOS), *N*-methyl pyrrolidone (NMP), ethanol, chloroform, hydrofluoric acid (HF), Tween-80, and glycol were purchased from Tianjin Kermel Chemical Reagent Co., Ltd. (China).

2.2. Fabrication of Homemade PVDF Substrates. To investigate the inherent properties of the possible formed coatings, we fabricated homemade PVDF membranes with few pores as substrates to avoid the interference of porous structure. In a typical approach, the casting solution of PVDF membrane was prepared by

DOI: 10.1021/acsami.5b00894
ACS Appl. Mater. Interfaces 2015, 7, 9534−9545

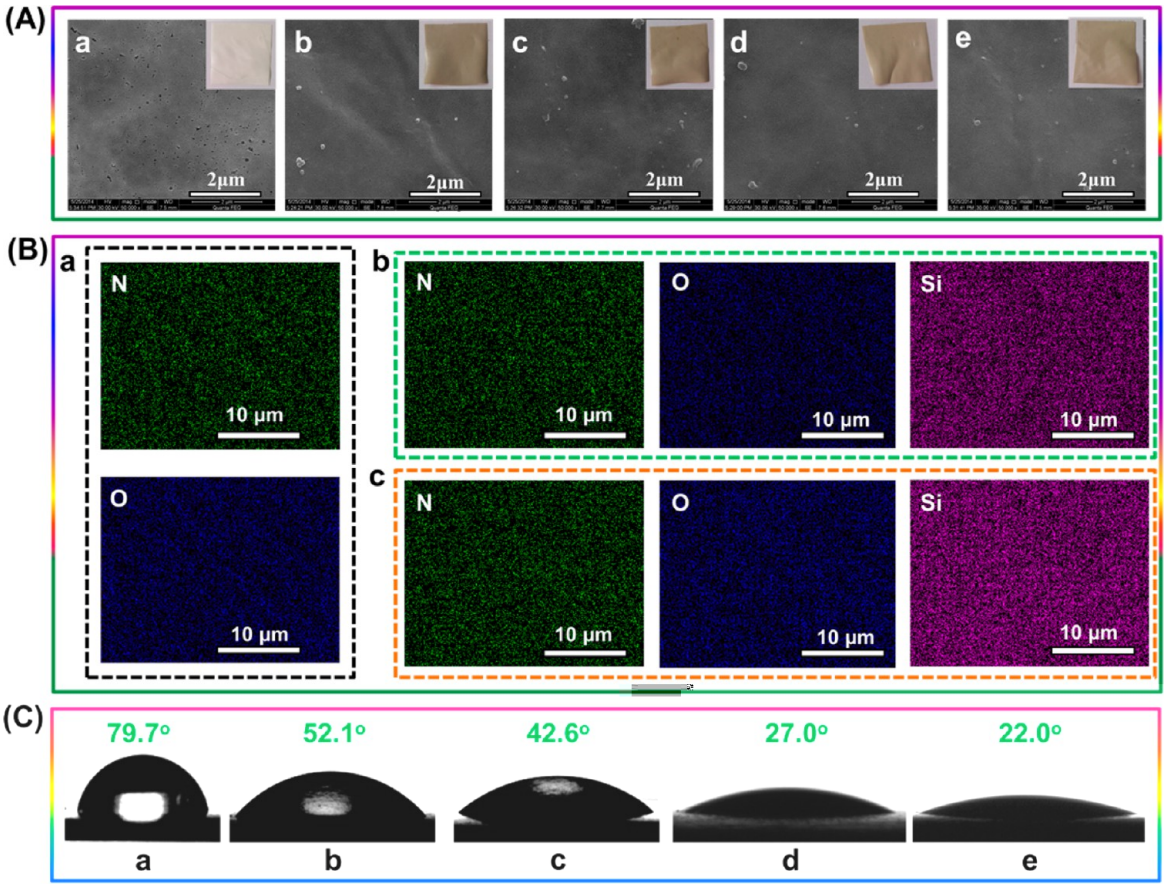

Figure 1. Characterization of the DA/TEOS-treated PVDF membranes. (A) SEM images and (C) water contact angles of (a) pristine PVDF substrate, PVDF substrate treated by (b) DA solution (2.0 mg mL^{-1}), and (c–e) DA/TEOS solution containing (c) 1.5, (d) 3.0, and (e) 6.0 mg mL^{-1} TEOS and 2.0 mg mL^{-1} DA for 9 h. The insets are corresponding photo images of pristine and modified PVDF substrates. (B) EDX mapping of (a) pristine PVDF substrate, and PVDF substrates treated by (b) 2.0 mg mL^{-1} of DA and 1.5 mg mL^{-1} TEOS and (c) 2.0 mg mL^{-1} DA and 6.0 mg mL^{-1} TEOS for 9 h. Green, blue, and pink dots indicate elemental N, O, and Si, respectively.

dissolving 16 g of PVDF in 84 g of *N*-methyl pyrrolidone (NMP). The solution was sealed and stored at 60 °C for more than 12 h to remove air bubbles, and casted on a glass plate using a doctor blade. Then the membrane was immediately immersed in a coagulant bath containing pure water at room temperature. After complete coagulation, the as-cast membrane was placed in a deionized water bath for solvent exchange. Subsequently, the homemade membranes (PVDF substrates) were carefully stored in water before usage.

2.3. Reaction Coating on Homemade PVDF Substrates. In a typical experiment, 0.2 g of dopamine hydrochloride was dissolved in 100 mL of HCl-Tris buffer solution (pH 8.5, 50 mM). After that, 25 mL of ethanol containing different amounts of TEOS (0.00, 0.15, 0.30, and 0.60 g) were added to the dopamine solution. Then PVDF substrate (membrane) (10 cm × 5 cm) was immediately immersed into the above solution for different durations (6, 9, and 12 h) at room temperature. Finally, the modified membrane was fully washed with deionized water and ethanol separately, and dried under vacuum.

2.4. High Hydrophilic Modification of Commercial Porous PVDF Microfiltration (MF) Membrane. We optimize the one-step process, and the reaction duration was decreased to 6 h and the amount of TEOS was increased to 0.9 g. Commercial PVDF microfiltration membrane with plentiful micropores was dealt with the optimized process for oily emulsion separation. The DA/TEOS-decorated porous membrane was fully washed with deionized water and ethanol separately, and dried under vacuum. In addition, we also prepared a DA-decorated porous MF membrane without adding TEOS for comparison.

2.5. Characterizations. Surface morphologies and the element mapping of pristine and modified PVDF substrates, as well as the PVDF MF membrane and carbon fiber with coatings before and after etching by HF, were characterized using scanning electron microscopy (SEM, S-4500, Hitachi, Japan) and energy-dispersive spectroscopy (EDS), respectively. (Note that it is very difficult to break up the commercial PVDF MF membrane by repeatedly bending in liquid nitrogen, thus the cross section of the MF membrane was obtained by torn through a gap in liquid nitrogen). Surface roughness was obtained by atomic force microscopy (Solver P47 AFM, Russia) in a tapping mode in the range of scanning area of 4 μm × 4 μm. The morphologies of pDA nanoparticles and hybrid nanoparticles before and after etching by HF were performed on transmission electron microscopy (Tecnai G2 F30, USA). The ATR-FTIR measurements were performed using a Spectrum One instrument (PerkinElmer, USA). XPS measurements were performed on an AXIS ULTRA DLD spectrometer (SHIMADZU, Japan). The weight ratio of silica and pDA in hybrid particles was determined with a thermal gravimetric analyzer (Q500, TA Instruments, New Castle, DE, USA) over a temperature range from room temperature to 1000 °C at a heating rate of 10 °C min^{-1} under atmosphere. The water contact angle and underwater–oil (chloroform) contact angle of pristine and modified surfaces were characterized by a contact angle measuring system (SL200 KB, USA). Deionized water and glycol were utilized to evaluate the surface energy (SE). The contact angle value was calculated by averaging over more than eight contact angle values at different sites. In each measurement, an approximate 2 μL droplet was dispensed onto the substrates. SE is the sum of polar and disperse parts. SE and its components are calculated by eq 1[43]

DOI: 10.1021/acsami.5b00894
ACS Appl. Mater. Interfaces 2015, 7, 9534–9545

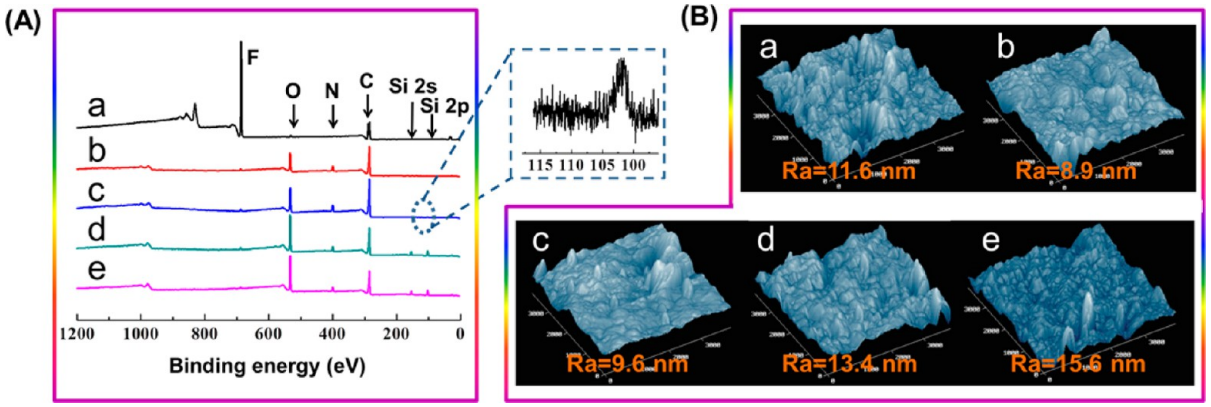

Figure 2. (A) XPS spectra and (B) AFM images of (a) pristine PVDF substrate, PVDF substrate treated by (b) DA solution (2.0 mg mL^{-1}) and (c–e) DA/TEOS solution containing (c) 1.5, (d) 3.0, and (e) 6.0 mg mL^{-1} TEOS and 2.0 mg mL^{-1} DA for 9 h. The scanning area of every sample is 4 μm × 4 μm.

Table 1. Elemental Composition of Different PVDF Substrates As Determined by XPS

	composition (at %)					atomic ratio			
membrane	C	F	O	N	Si	N/C	O/C	Si/C	O/Si
pristine PVDF	51.0	49.0							
PVDF/pDA	73.4	0.7	19.1	6.8		0.09	0.26		
PVDF/(DA-TEOS 0.15)	73.8	1.0	18.1	6.7	0.4	0.09	0.25	0.01	49.81
PVDF/(DA-TEOS 0.30)	57.7	1.1	27.2	4.9	9.1	0.09	0.47	0.16	2.96
PVDF/(DA-TEOS 0.60)	55.3	0.6	29.2	4.6	10.3	0.08	0.53	0.19	2.82

$$\gamma_l(1+\cos\theta)=\frac{4\gamma_s^d\gamma_l^d}{\gamma_s^d+\gamma_l^d}+\frac{4\gamma_s^p\gamma_l^p}{\gamma_s^p+\gamma_l^p} \quad (1)$$

where γ refers to surface energy, the subscripts l and s refer to liquid and solid, and the superscripts d and p refer to dispersive and polar components, respectively. θ refers to contact angles between ordinary liquids (H_2O or glycol) and the substrates.[43]

2.6. Emulsion separation experiments. Twenty milliliters of chloroform was added into 980 mL of deionized water with 15 mg of Tween-80 as emulsifier; the solution was then stirred under 1000 rpm for 3 h. The droplet sizes are in the range of 4 to 14 μm under optical microscopy observation. Pure water flux, oil-in-water emulsion separation and antifouling experiments of porous PVDF MF membrane was tested by a vacuum driven filtration system at 0.09 MPa (vacuum degree −0.09 MPa). Besides, we also test the flux of oil-in-water emulsion driven solely by gravity (about 120 mm emulsion column). The flux of the porous PVDF MF membrane was obtained by eq 2

$$\text{flux}=\frac{V}{At} \quad (2)$$

Where flux is the pure water or filtrate flux (L m^{-2} h^{-1}), V is the permeate volume measured (L), A is the membrane active area (m^2), and t is the permeation time (h). The active area of porous membrane is 17.34 cm^2.

2.7. Long-Term Stability Test. The highly hydrophilic and underwater superoleophobic stability of the modified MF membrane was investigated by long-term washing treatment with water and repeated bending tests in liquid nitrogen. (It is very difficult to break up the commercial PVDF MF membrane by repeatedly bending in liquid nitrogen. Thus, we can determine the stability of the decorated MF membrane by repeated bending in liquid nitrogen.) Both water CA and underwater–oil CA of the decorated MF membrane were obtained by a contact angle measuring system (SL200 KB, USA) to evaluate stability of the membrane.

3. RESULTS AND DISCUSSION

PDA layers have been shown to form firmly on PVDF substrates.[20,26,44] However, coating formation on PVDF substrates in the presence of DA and TEOS remains unknown. To investigate the inherent properties of the possible formed coatings, homemade PVDF membranes with few pores were fabricated as substrates to avoid the interference of porous structure. Images in Figure 1A show the color change between pristine and modified PVDF membranes. The colors of DA/TEOS and pure DA-treated membranes are similar, implying the possible formation of pDA coatings on PVDF substrates treated by DA/TEOS mixtures. Moreover, after being treated by either DA or DA/TEOS, nanopores on the surface of pristine PVDF substrates disappeared, which may due to the possible coating formed on those PVDF substrates.

EDX mapping and ATR-FTIR of modified PVDF substrates shown in Figure 1B and Figure S1 in the Supporting Information, respectively, reveal homogeneous dispersion of N, O, and Si elements across the surfaces of DA/TEOS-treated PVDF substrates. These results confirm the formation of coatings on the DA/TEOS-treated PVDF membranes. The presence of N and O elements was ascribed to pDA, whereas Si and O elements were derived from the hydrolysis product of low-cost TEOS (Figure S1 in the Supporting Information). Interestingly, these coatings formed with different content of TEOS did not show obvious differences in SEM images and EDX mappings. Nevertheless, the drastic decline in water contact angle (CA) from 42.6 to 22.0° denoted different properties of these coatings (Figure 2C). The water CAs of the coatings formed in DA/TEOS solution were much lower compared to pure pDA coatings (52.1°), and attributed to drastic improvements in hydrophilicity of PVDF substrates. Hydrophilicity of these coatings could also be controlled by adjusting the TEOS concentration. Higher TEOS content

DOI: 10.1021/acsami.5b00894
ACS Appl. Mater. Interfaces 2015, 7, 9534–9545

gradually reduced the water CA of substrates and rendered them tunable wettability toward high hydrophilicity. Without DA, the water CA of TEOS-treated PVDF substrate remained similar to those of pristine substrates, demonstrating the crucial role of DA in immobilizing TEOS hydrolysis products on porous PVDF substrates. Therefore, both TEOS and DA are mandatory in our strategy for overcoming the inherent hydrophobicity of PVDF to achieve high hydrophilicity and underwater superoleophobicity.

XPS and AFM were performed to further examine the cause of such tunable hydrophilicity, which is crucial for the elegant designing of novel hybrid coatings toward high hydrophilicity. For DA/TEOS-treated PVDF membranes, all F 1s peaks of original PVDF materials disappeared due to the coatings. Instead, new peaks (O 1s, N 1s, Si 2s, and 2p peaks) were observed, and the N/C ratio is about 0.8−0.9 consistent with the values of pDA reported by others,[26] demonstrating the coatings are composed of pDA and silica (Figure 2A, Figure S2 in the Supporting Information, and Table 1). As shown in Table 1, the silica content on the surface of organic−inorganic coatings is different and could be controlled by adjusting the amount of TEOS in DA/TEOS solution. For example, Si content on the surface of organic−inorganic coatings could be significantly enhanced by more than 2300% by doubling TEOS content in DA/TEOS solution, while water CA correspondingly decreased from 42.6 to 27°. Further increment of TEOS content slightly improved Si content on the surface and reduced water CA. These results attributed the drastic improvement of hydrophilicity to the higher silica content on the top surface of organic−inorganic coatings. The influence of silica content on hydrophilicity is further elucidated by surface energy characterizations (Table 2). Compared with pure pDA

Table 2. Contact Angles and Surface Energy of PVDF Substrates Modified with Varying Amounts of Dopamine (DA) and TEOS for 9 h

samples	contact angle (deg)		surface-energy components (mJ m^{-2})		
	water	glycol	γ_L	γ_L^p	γ_L^d
PVDF	79.7 ± 0.7	51.1 ± 0.6	33.2	7.0	26.2
PVDF/DA	52.1 ± 0.6	23.0 ± 2.1	47.5	31.2	16.3
PVDF/TEOS 0.60	80.1 ± 0.5	50.8 ± 0.8	33.6	6.5	27.1
PVDF/(DA-TEOS 0.15)	42.6 ± 0.8	18.2 ± 2.0	55.9	45.4	10.5
PVDF/(DA-TEOS 0.30)	27.0 ± 0.9	13.1 ± 2.8	73.1	68.7	4.4
PVDF/(DA-TEOS 0.60)	22.0 ± 1.5	10.4 ± 2.9	77.8	74.4	3.5

coating, the organic−inorganic coatings possessed higher total surface energies that gradually increased with silica content. The most drastic increase lies in the polar component of silica,[43] highlighting the vital role of silica location within organic−inorganic coatings for tuning surface hydrophilicity. Besides, with the increase in TEOS amount, there is only a slight increase in surface roughness for these coatings, indicating that the significant improvement of hydrophilicity is mainly due to the incorporation of hydrophilic silica (Figure 2B). The water contact angles of DA/TEOS-treated membrane with different reaction coating duration are also demonstrated in Table 3. Note that the water contact angle gradually increase with the reaction coating duration, and finally a water contact angle similar to that of DA-treated membrane was obtained.

Table 3. Water Contact Angles of PVDF Substrates Modified with Varying Amounts of Dopamine (DA) and TEOS for Different Reaction Coating Duration

content		water contact angle (deg)		
DA (g)	TEOS (g)	6 h	9 h	12 h
0.20	0.00	61.0 ± 0.5	52.1 ± 0.6	40.6 ± 0.7
	0.15	29.3 ± 0.7	42.6 ± 0.8	40.0 ± 0.9
	0.30	20.3 ± 1.5	27.0 ± 0.9	31.7 ± 1.5
	0.60	18.5 ± 1.8	22.0 ± 1.5	30.9 ± 1.0

The various hydrophilicity of these coating may result from the different distribution of hydrophilic silica which is important for us to further disclose the nature of the coatings. The distribution of silica in these coatings should be similar to that in nanoparticles formed in the same mixed solution. Thus, thermo gravimetric analysis (TGA) and TEM images of the nanoparticles formed in DA/TEOS solution are shown. TGA results of nanoparticles formed in situ in DA/TEOS solutions (Figure 3) showed that the silica content in nanoparticles

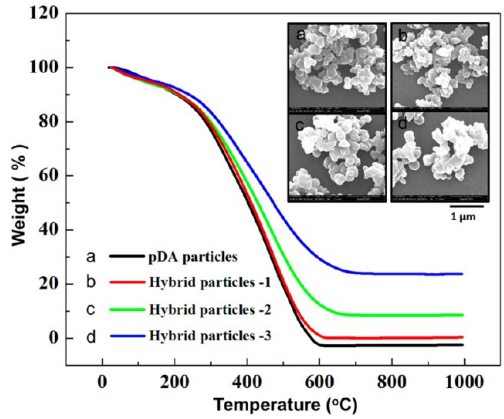

Figure 3. TGA and SEM images (inset) of (a) pure pDA particles and (b−d) hybrid particles formed in DA/TEOS solution containing (b) 1.5, (c) 3.0, and (d) 6.0 mg mL^{-1} TEOS and 2.0 mg mL^{-1} DA for 9 h.

gradually improved with the increase of TEOS content, which is consistent with the previous results of organic−inorganic coatings. The TEM images of pDA nanoparticles and nanoparticles formed in different DA/TEOS solution are shown in Figure 4A. It seems that there is no obvious difference between those nanoparticles, and it is difficult to observe the distribution of silica in the nanoparticles via these images. Thus, hydrofluoric acid (HF) is utilized to etch those nanoparticles for clarify the silica distribution, and the TEM images of these nanoparticles after HF etching are shown in Figure 4B. According to the TEM images of the nanoparticles before and after HF etching, we can further confirm the nanoparticles are hybrid and are composed of pDA and silica. Interestingly, these nanoparticles exhibit entirely different distribution of silica when varying the TEOS amounts in DA/TEOS solution. The structure of the nanoparticles changes from core−shell structure to dandelion structure with the increase in TEOS amount in DA/TEOS solution. For the nanoparticles with core−shell structure formed at the lower TEOS amount, the core should be silica that had been etched by HF, whereas the shell should be a pDA layer that can not be etched by HF. This indicates that most silica is in the inner of these hybrid particles if the amount of TEOS is low. Note that

DOI: 10.1021/acsami.5b00894
ACS Appl. Mater. Interfaces 2015, 7, 9534−9545

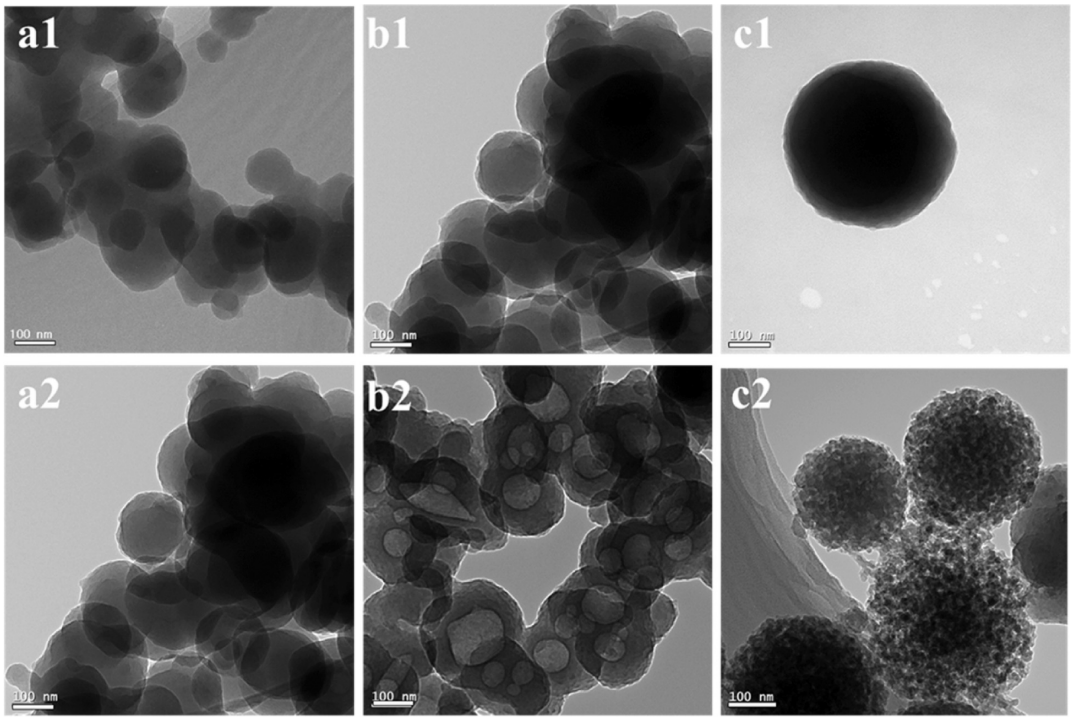

Figure 4. TEM images (1, before HF etching; 2, after HF etching) of (a) pure pDA particles and (b, c) hybrid particles formed in DA/TEOS solution containing 2.0 mg mL^{-1} DA and (b) 1.5 and (c) 6.0 mg mL^{-1} TEOS and for 9 h.

the surface of these nanoparticles become rough after HF etching, indicating there is still a little silica on the surface of these nanoparticles although most silica are in the inner of these hybrid particles as the core. It explains the only slight improvement of hydrophilicity for the PVDF membrane treated by DA/TEOS solution at the lower TEOS content. For the hybrid nanoparticles with dandelion structure formed at the higher TEOS amount, the silica is uniformly distributed from the inner to the outer surface of the hybrid particles. Note that the surface of these nanoparticles after HF etching is much rougher than those nanoparticles formed at the lower TEOS amount, indicating that there is still much silica on the outer surface of these nanoparticles. Based on a series of water contact angles, EDX mapping and the XPS results of different coatings, as well as the TEM images of nanoparticles before and after HF etching, a possible sketch map of these coatings with different hydrophilicity and corresponding distribution of silica are shown in Scheme 2. The little TEOS amount in DA/TEOS

Scheme 2. Illustration of the Possible Distribution of Silica in Hybrid Coatings with (a) the Little TEOS and (b) Increasing Amounts of TEOS in DA/TEOS Solution

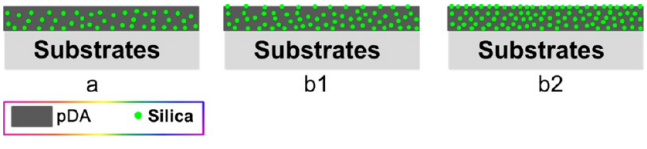

solution and the long reaction coating duration may make most silica in the inner of the coatings (Scheme 2a). In contrast, with the increase in TEOS in the DA/TEOS solution, there may be much silica on the outer surface of the coatings (Scheme 2b), and the plentiful silica on the outer surface is beneficial for significantly improving the hydrophilicity of hybrid coatings.

Optimized hybrid coatings were coated on commercial porous PVDF microfiltration (MF) membranes for oil/water separation applications. According to the EDX mappings of the DA/TEOS-treated MF membrane shown in Figure 5, the elements N, O, and Si disperse homogeneously on the top surface and cross-section of the membrane. Furthermore, as shown in Figure 6 and Figure S3 in the Supporting Information, few nanoparticles can be observed on either the top surface or cross section of the DA/TEOS-treated porous MF membrane, implying the elements N, O and Si are derived from the hybrid coatings on membrane rather than nanoparticles that may trapped in the membrane. The variant wetting behaviors of pristine, DA, and DA/TEOS-decorated commercial porous MF membrane are illustrated in Figure 7. Notably, the DA/TEOS-decorated MF membrane can be easily soaked through by water drop, whereas both the pristine and DA-decorated commercial PVDF MF membrane are hard to soak. It indicates our optimized hybrid coatings can endow hydrophobic MF membrane with special wettability. To accurately measure the different wettability of those membranes, we show the water contact angles and their changes over time in Figure 8. The inherent high hydrophobic and poor wettability of the commercial porous PVDF MF membrane can be demonstrated by the large and nearly invariable water CA (~120°). For DA-decorated PVDF MF membrane, it is still hydrophobic (~100°) and only a little decline of water CA was observed even after 30s, disclosing the limitation of pure pDA coating in improving wettability of hydrophobic membrane. By contrast, the water contact angle of the DA/TEOS-treated MF membrane is about 12°, exhibiting high hydrophilicity. Moreover, the water droplet on the DA/TEOS-decorated PVDF MF membrane surface can spread easily and permeated into the membrane within 2s, and a water contact angle of about 0° was observed. The high hydrophilicity of the MF membrane should be derived from the silica on the outer

DOI: 10.1021/acsami.5b00894
ACS Appl. Mater. Interfaces 2015, 7, 9534−9545

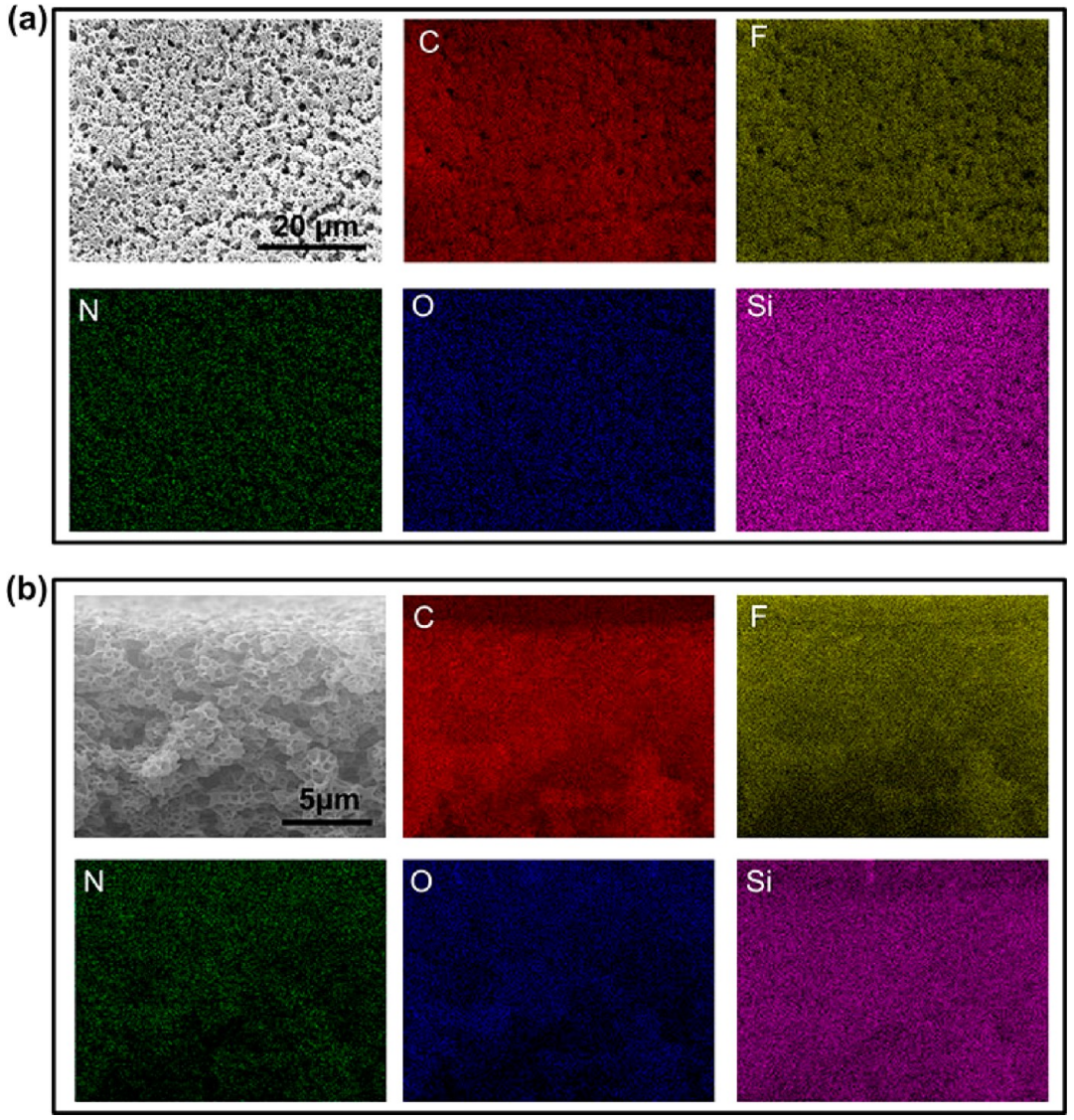

Figure 5. SEM and EDX mapping of (a) top surface and (b) cross-section of PVDF MF membrane treated by DA/TEOS solution containing 2.0 mg mL^{-1} DA and 9.0 mg mL^{-1} TEOS for 6 h. Red, yellow, green, blue, and pink dots indicate signals of C, F, N, O, and Si, respectively.

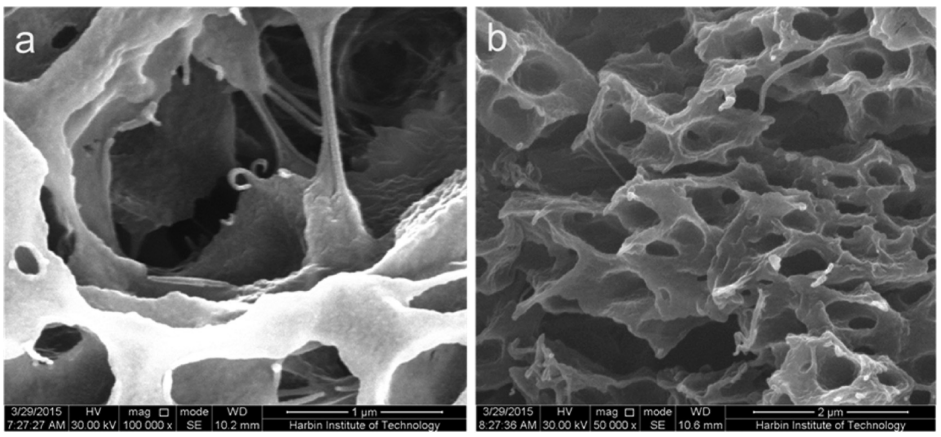

Figure 6. SEM images of the (a) top surface and (b) cross-section of the PVDF MF membrane treated by DA/TEOS solution containing 2.0 mg mL^{-1} DA and 9.0 mg mL^{-1} TEOS for 6 h.

surface of the hybrid coatings just as the sketch map illustrated in Scheme 2b. To confirm this point, we show the water contact angles before and after HF etching in Figure S4 in the Supporting Information. After being etched by HF, the water contact angle of the DA/TEOS-treated MF membrane change from 12° to about 105°, which is similar to that of pure DA-

DOI: 10.1021/acsami.5b00894
ACS Appl. Mater. Interfaces 2015, 7, 9534−9545

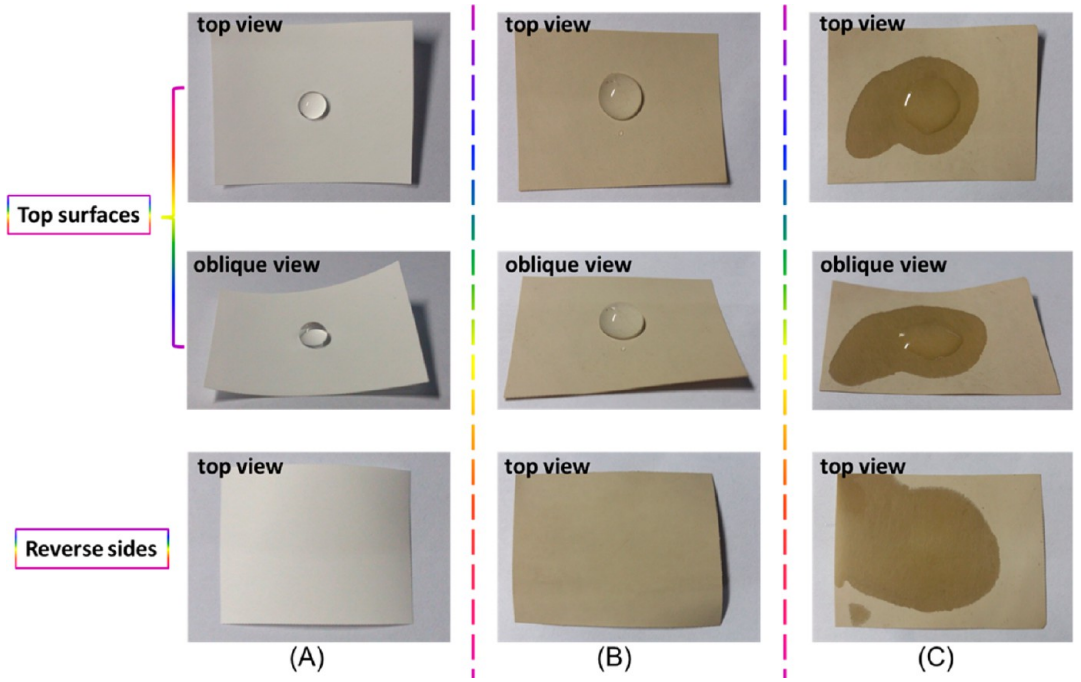

Figure 7. Photographs of a large drop of water (about 0.2 mL) on (A) pristine PVDF MF membrane, (B) PVDF MF membrane treated by DA solution (2.0 mg mL^{-1}) for 6 h, and (C) PVDF MF membrane treated by DA/TEOS solution containing 2.0 mg mL^{-1} of DA and 9.0 mg mL^{-1} of TEOS for 6 h. Those images (top view, oblique view, and reverse sides) for every kind of membrane are taken in less than 10 s.

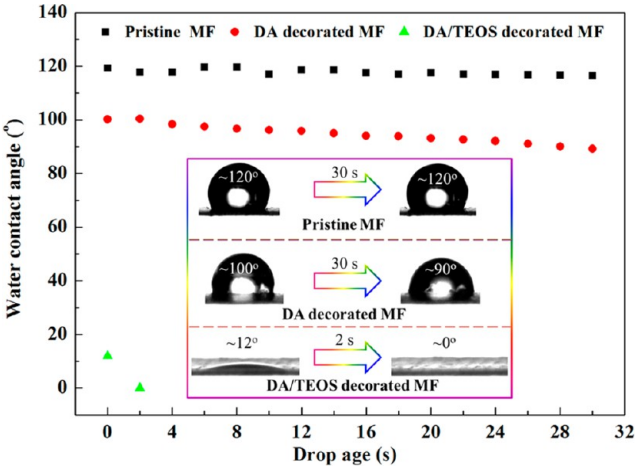

Figure 8. Water contact angles of pristine, DA (2.0 mg mL^{-1}) decorated, and DA/TEOS (DA 2.0 mg mL^{-1} and TEOS 9.0 mg mL^{-1}) decorated PVDF MF membranes with different drop age. The inset is photographs of a water droplet on different MF membranes. (The water droplet is about 2 μL).

treated MF membrane. Besides, the morphologies of the DA/TEOS-treated membrane (top surface) before and after HF etching are shown in Figure S5 in the Supporting Information. However, because of the rugged surface and limited electrical conductivity, the images are not so clear that some fine changes may not be observed only by the SEM images. We notice that the smooth, electrical conductivity and cylindrical surface of pristine carbon fiber may help us to clearly observe the fine change of the coatings. Thus, we use same DA/TEOS solution to treat carbon fiber (T 700SC-12000-50C) and observed the fine variation of the coatings on carbon fiber before and after being etched by HF. The SEM images of DA/TEOS-treated carbon fiber before and after HF etching, as well as the pristine carbon fiber, are shown in Figure S6 in the Supporting Information. It is obvious that the coating on carbon fiber becomes much rough after being etched by HF, indicating the existence of silica on the outer surface of the hybrid coatings just as that in sketch map shown in Scheme 2b. Therefore, the high hydrophilicity of the DA/TEOS-treated MF membrane should be attributed to the silica on the outer surface of the hybrid coatings.

Furthermore, the underwater–oil CA of this membrane is about 155°, demonstrating underwater superoleophobicity (Figure 9A). The DA/TEOS-decorated commercial MF membrane also showed excellent antiadhesion to oil. As shown in Figure 9B, an oil droplet was forced to adequately

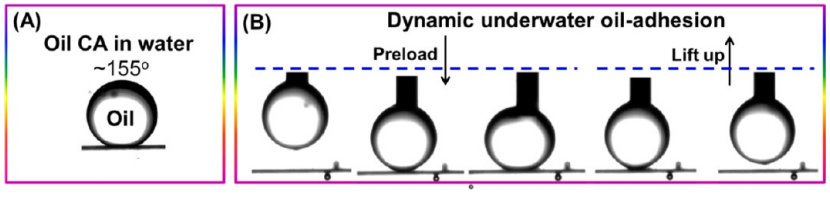

Figure 9. (A) Underwater–oil contact angle and (B) dynamic underwater–oil-adhesion of the PVDF MF membrane treated by DA/TEOS solution containing 2.0 mg mL^{-1} of DA and 9.0 mg mL^{-1} of TEOS for 6 h.

DOI: 10.1021/acsami.5b00894
ACS Appl. Mater. Interfaces 2015, 7, 9534–9545

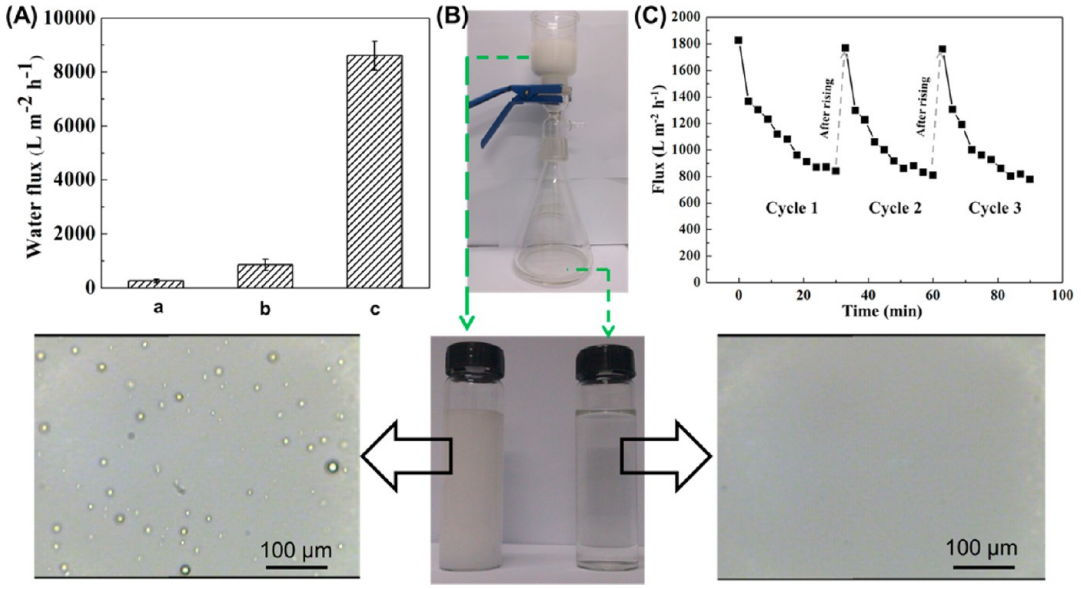

Figure 10. (A) Pure water flux of (a) pristine PVDF MF, (b) PVDF MF membrane treated with DA solution (2.0 mg mL^{-1}), and (c) PVDF MF membrane treated by DA/TEOS solution containing 2.0 mg mL^{-1} of DA and 9.0 mg mL^{-1} of TEOS for 6 h. (B) Photograph of oil-in-water emulsion separation driven solely by gravity and separation results of oil-in-water emulsions by DA/TEOS-treated membrane. (C) Flux recovery in the separation of oil-in-water emulsion over three cycles under 0.09 MPa.

contact the membrane surface and then lifted up. During the lifting process, the oil droplet remained spherical and no obvious deformation was observed, revealing the low-oil adhesion of the DA/TEOS-decorated MF membrane. Because of the underwater low adhesion of oil, the oil droplet on the DA/TEOS-treated MF membrane can easily roll off the membrane surface, and the rolling angle is as low as 5° (Video S1 in the Supporting Information). As shown in Figure S7 in the Supporting Information, the membrane shows high adhesion of water (under oil), indicating the higher affinity between water and the silica than that between oil and silica, which can explain the underwater superoleophobicity and low oil adhesion ability of our membrane.[17,45] The underwater superoleophobicity and low oil adhesion ability of the membrane treated with optimized hybrid coating provided a good basis for oil-in-water separation with antifouling performance.

Significantly, the pure water flux of DA/TEOS-treated porous membrane at 0.9 bar is as high as 8606 L m^{-2} h^{-1}, 34 times and 10 times higher than that of pristine and DA-decorated MF membranes, respectively (Figure 10A). In fact, the significant improved water flux can be explained by the almost unchanged pore size and high hydrophilicity of the DA/TEOS-treated MF membrane. In fact, both the pure pDA coating and hybrid coating on membrane are very thin, and the hybrid coatings should be only about dozens of nanometers according to the SEM images of the cross section of PVDF membrane (Figure S8 in the Supporting Information) and the TEM images of the copper grid coated with these coatings (Figure S9 in the Supporting Information). The thickness value of the hybrid coating is similar to that of pure pDA coating that had been reported by other researchers.[26,46] Thanks to the thinness of these coating, the pore size of PVDF MF membrane decorated by these coatings remains almost unchanged (Figure S10 in the Supporting Information). Under this circumstance, the hydrophilicity of the membrane plays an extremely important role on deciding the water flux. For DA/TEOS-treated MF membrane, the hydrophilicity of the membrane is much better than that of the DA-treated MF membrane. The significantly enhanced hydrophilicity can drastically decrease the water permeation resistance and make water permeate much more rapidly through the membrane under same pressure.[21,24,30] Thus, the DA/TEOS-treated MF membrane has much higher water flux than the DA-treated MF membrane. Thanks to the ultrahigh water flux of our membrane, the separation of oil-in-water emulsions could be gravity-driven (Figure 10B), and the pure water flux of DA/TEOS-treated membrane for such an operation was about 140 L m^{-2} h^{-1}, comparable to that of many ultrafiltration membranes under extra pressure.[20] Such separation performance is extremely attractive for high efficiency, low carbon footprint separations. Figure 10B showed that the DA/TEOS-decorated porous membrane removed oil emulsions from a milky white oil-in-water emulsion (Left) to yield a clear solution of water (Right). Before filtration, the milky white oil-in-water emulsion contained 4−14 μm oil droplets. After filtration, the filtrate was transparent and no oil droplets were observed, illustrating that oil had been successfully removed from the oily water. To better evaluate the antifouling performance of the DA/TEOS-treated membrane, we carried out a three-cyclic filtration test under constant pressure (about 0.09 MPa) (Figure 10C). The filtration time is 30 min and the amount (volume) of emulsion passing through the membrane is about 900−1000 mL for every cycle. And then, the membrane surface is washed by water to remove the oil cake on the membrane for next cycle. Different from the flux decline driven solely by gravity Figure S11 in the Supporting Information), the flux declines sharply in the first 3 min and then decreases slowly under the constant pressure (about 0.09 MPa). Such phenomenon may due to the faster formation of "oil drops cake" under much high pressure.[5,15,40,47] Note that the flux of the DA/TEOS-treated membrane almost recovers the initial flux after rinsing by water, exhibiting excellent flux recovery. The antifouling performance of the DA/TEOS-decorated membrane should be ascribed to the retentive superoleophobicity and low-adhesion of oil under

DOI: 10.1021/acsami.5b00894
ACS Appl. Mater. Interfaces 2015, 7, 9534−9545

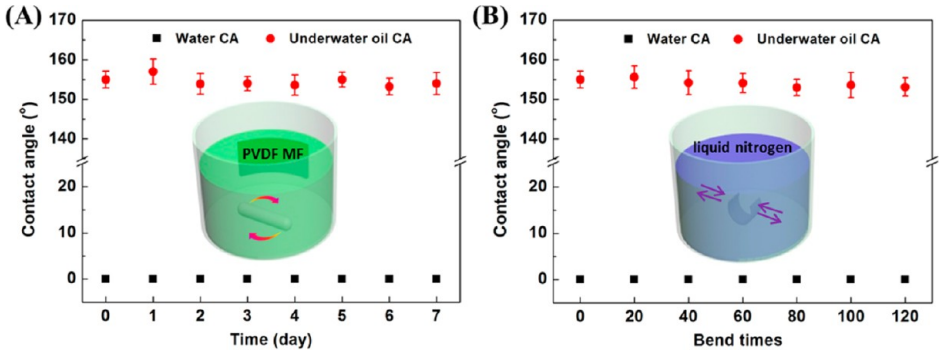

Figure 11. Water CA and underwater−oil CA of the DA/TEOS-decorated MF membrane after being (A) rinsed with water using a magnetic stirrer and (B) bent repeatedly in liquid nitrogen. The two insets are the corresponding schematics of the two different processes. The water contact angle was recorded after the water droplet on membrane after 2 s.

water containing surfactant (Figure S12 and Video S2 in the Supporting Information).

The stable and high hydrophilicity, and underwater superoleophobicity are very important for the porous PVDF membrane to separate the oil-in-water emulsion with high efficiency in long-term operations.[25] Therefore, both long washing treatment and repeated bending in liquid nitrogen were carried out to investigate the stability of the DA/TEOS-decorated PVDF MF membrane (Figure 11). The membrane showed underwater−oil CA of above 150° during the long washing process (Figure 11A), indicating that it could withstand continuous and drastic scouring without losing underwater superoleophobicity. Moreover, as shown in Figure 11B, the porous PVDF membrane retained underwater superoleophobicity even after repeated bending in liquid nitrogen, disclosing the excellent durability of the hybrid coating.

4. CONCLUSIONS

In conclusion, a novel and economical one-step method to fabricate "water-removing" porous polymer membrane for highly efficient and eco-friendly oil-in-water emulsion separation is discovered via simultaneous polymerization of DA and hydrolysis of TEOS. In this mussel-inspired one-step process, hybrid coatings were formed. By finely tuning TEOS content and reaction duration, the mussel-inspired hybrid coating rendered PVDF microfiltration membranes with exceptional high hydrophilicity and underwater superoleophobicity with low oil adhesion, endowing the membranes with ultrahigh pure water flux (8606 L m^{-2} h^{-1} only under 0.9 bar), and gravity-driven oily emulsion separation functions (filtrate flux of 140 L m^{-2} h^{-1}) with excellent antifouling ability to oil. Even after long-term water rinsing or even repeated bending in liquid nitrogen, the modified PVDF microfiltration membrane still retained high hydrophilicity and underwater superoleophobicity, disclosing the excellent stability of the hybrid coatings.

■ ASSOCIATED CONTENT

Supporting Information

ATR-FTIR spectra of pristine and modified PVDF substrates, O 1s spectrum of different PVDF substrates, SEM images of the top surface and cross section of the modified MF membrane, water contact angles and SEM images of the DA/TEOS-treated MF membrane before and after etching by HF, SEM images of DA/TEOS-treated carbon fiber before and after etching by HF, under oil−water contact angle and water-adhesion images of the DA/TEOS-treated MF membrane, SEM images of the cross-section of DA/TEOS-treated PVDF substrate, TEM images of DA/TEOS-treated copper grid, flux recovery in the separation (driven solely by gravity) of oil-in-water emulsion over four cycles, and underwater (containing surfactant) oil contact angle of the DA/TEOS-treated MF membrane. Video S1 is the underwater−oil rolling process on the DA/TEOS-treated MF membrane, and Video S2 shows the underwater (containing surfactant) low oil-adhesion of the PVDF MF membrane treated by DA/TEOS. This material is available free of charge via the Internet at http://pubs.acs.org.

■ AUTHOR INFORMATION

Corresponding Authors

*E-mail: cherhon.lau@csiro.au.
*E-mail: shaolu@hit.edu.cn.

Notes

The authors declare no competing financial interest.

■ ACKNOWLEDGMENTS

This work was supported by National Natural Science Foundation of China (21177032, U1462103), Program for New Century Excellent Talents in University (NCET-11-0805), the Fundamental Research Funds for the Central Universities (Grant HIT.BRETIV.201307), Harbin Science and Technology Innovation Talent Funds (2014RFXXJ028), and State Key Laboratory of Urban Water Resource and Environment (Harbin Institute Technology) (2014DX05).

■ REFERENCES

(1) Liu, K.; Yao, X.; Jiang, L. Recent Developments in Bio-inspired Special Wettability. *Chem. Soc. Rev.* **2010**, *39*, 3240−3255.
(2) Feng, X. J.; Jiang, L. Design and Creation of Superwetting/Antiwetting Surfaces. *Adv. Mater.* **2006**, *18*, 3063−3078.
(3) Duong, P. H.; Chung, T. S.; Wei, S.; Irish, L. Highly Permeable Double-skinned Forward Osmosis Membranes for Anti-fouling in the Emulsified Oil-water Separation Process. *Environ. Sci. Technol.* **2014**, *48*, 4537−4545.
(4) Zhang, S.; Wang, P.; Fu, X.; Chung, T. S. Sustainable Water Recovery From Oily Wastewater via Forward Osmosis-membrane Distillation (FO-MD). *Water. Res.* **2014**, *52*, 112−121.
(5) Zhu, Y.; Wang, D.; Jiang, L.; Jin, J. Recent Progress in Developing Advanced Membranes for Emulsified Oil/water Separation. *NPG Asia Mater.* **2014**, *6*, e101.
(6) Zhu, Q.; Pan, Q. Mussel-inspired Direct Immobilization of Nanoparticles and Application for Oil-Water Separation. *ACS Nano* **2014**, *8*, 1402−1409.

DOI: 10.1021/acsami.5b00894
ACS Appl. Mater. Interfaces 2015, 7, 9534−9545

(7) Xue, Z.; Wang, S.; Lin, L.; Chen, L.; Liu, M.; Feng, L.; Jiang, L. A Novel Superhydrophilic and Underwater Superoleophobic Hydrogel-Coated Mesh for Oil/Water Separation. *Adv. Mater.* **2011**, *23*, 4270−4273.
(8) Chen, N.; Pan, Q. Versatile Fabrication of Ultralight Magnetic Foams and Application for Oil-water Separation. *ACS Nano* **2013**, *7*, 6875−6883.
(9) Calcagnile, P.; Fragouli, D.; Bayer, I. S.; Anyfantis, G. C.; Martiradonna, L.; Cozzoli, P. D.; Cingolani, R.; Athanassiou, A. Magnetically Driven Floating Foams for the Removal of Oil Contaminants from Water. *ACS Nano* **2012**, *6*, 5413−5419.
(10) Pavia-Sanders, A.; Zhang, S.; Flores, J. A.; Sanders, J. E.; Raymond, J. E.; Wooley, K. L. Robust Magnetic/polymer Hybrid Nanoparticles Designed for Crude Oil Entrapment and Recovery in Aqueous Environments. *ACS Nano* **2013**, *7*, 7552−7561.
(11) Lee, M. W.; An, S.; Latthe, S. S.; Lee, C.; Hong, S.; Yoon, S. S. Electrospun Polystyrene Nanofiber Membrane with Superhydrophobicity and Superoleophilicity for Selective Separation of Water and Low Viscous Oil. *ACS Appl. Mater. Interfaces* **2013**, *5*, 10597−10604.
(12) Xue, Z. X.; Cao, Y. Z.; Liu, N.; Feng, L.; Jiang, L. Special Wettable Materials for Oil/water Separation. *J. Mater. Chem. A* **2014**, *2*, 2445−2460.
(13) Gao, S. J.; Shi, Z.; Zhang, W. B.; Zhang, F.; Jin, J. Photoinduced Superwetting Single-walled Carbon Nanotube/TiO(2) Ultrathin Network Films for Ultrafast Separation of Oil-in-water Emulsions. *ACS Nano* **2014**, *8*, 6344−6352.
(14) Liu, K.; Jiang, L. Multifunctional Integration: From Biological to Bio-inspired Materials. *ACS Nano* **2011**, *5*, 6786−6790.
(15) Zhang, W.; Zhu, Y.; Liu, X.; Wang, D.; Li, J.; Jiang, L.; Jin, J. Salt-induced Fabrication of Superhydrophilic and Underwater Superoleophobic PAA-g-PVDF Membranes for Effective Separation of Oil-in-water Emulsions. *Angew. Chem., Int. Ed.* **2014**, *53*, 856−860.
(16) Lu, Z.; Gao, C.; Zhang, Q.; Chi, M.; Howe, J. Y.; Yin, Y. Direct Assembly of Hydrophobic Nanoparticles to Multifunctional Structures. *Nano Lett.* **2011**, *11*, 3404−3412.
(17) Gao, X.; Xu, L. P.; Xue, Z.; Feng, L.; Peng, J.; Wen, Y.; Wang, S.; Zhang, X. Dual-scaled Porous Nitrocellulose Membranes with Underwater Superoleophobicity for Highly Efficient Oil/water Separation. *Adv. Mater.* **2014**, *26*, 1771−1775.
(18) Liu, Q.; Patel, A. A.; Liu, L. Superhydrophilic and Underwater Superoleophobic Poly(sulfobetaine methacrylate)-grafted Glass Fiber Filters for Oil-water Separation. *ACS Appl. Mater. Interfaces* **2014**, *6*, 8996−9003.
(19) Gondal, M. A.; Sadullah, M. S.; Dastageer, M. A.; McKinley, G. H.; Panchanathan, D.; Varanasi, K. K. Study of Factors Governing Oil-water Separation Process Using TiO(2) Films Prepared by Spray Deposition of Nanoparticle Dispersions. *ACS Appl. Mater. Interfaces* **2014**, *6*, 13422−13429.
(20) Shao, L.; Wang, Z. X.; Zhang, Y. L.; Jiang, Z. X.; Liu, Y. Y. A Facile Strategy to Enhance PVDF Ultrafiltration Membrane Performance via Self-polymerized Polydopamine Followed by Hydrolysis of Ammonium Fluotitanate. *J. Membr. Sci.* **2014**, *461*, 10−21.
(21) Kang, G. D.; Cao, Y. M. Application and Modification of Poly(vinylidene fluoride) (PVDF) Membranes − A review. *J. Membr. Sci.* **2014**, *463*, 145−165.
(22) Shao, L.; Cheng, X.; Wang, Z.; Ma, J.; Guo, Z. Tuning the Performance of Polypyrrole-based Solvent-resistant Composite Nanofiltration Membranes by Optimizing Polymerization Conditions and Incorporating Graphene Oxide. *J. Membr. Sci.* **2014**, *452*, 82−89.
(23) Tao, M.; Xue, L.; Liu, F.; Jiang, L. An Intelligent Superwetting PVDF Membrane Showing Switchable Transport Performance for Oil/water Separation. *Adv. Mater.* **2014**, *26*, 2943−2948.
(24) Liu, F.; Hashim, N. A.; Liu, Y.; Abed, M. R. M.; Li, K. Progress in the Production and Modification of PVDF Membranes. *J. Membr. Sci.* **2011**, *375*, 1−27.
(25) Wang, Y.; Shi, Y.; Pan, L.; Yang, M.; Peng, L.; Zong, S.; Yu, G. Multifunctional Superhydrophobic Surfaces Templated from Innately Microstructured Hydrogel Matrix. *Nano Lett.* **2014**, *14*, 4803−4809.
(26) Lee, H.; Dellatore, S. M.; Miller, W. M.; Messersmith, P. B. Mussel-inspired Surface Chemistry for Multifunctional Coatings. *Science* **2007**, *318*, 426−430.
(27) Liu, Y.; Ai, K.; Lu, L. Polydopamine and Its Derivative Materials: Synthesis and Promising Applications in Energy, Environmental, and Biomedical Fields. *Chem. Rev.* **2014**, *114*, 5057−5115.
(28) Wang, Z.-X.; Lau, C.-H.; Zhang, N.-Q.; Bai, Y.-P.; Shao, L. Mussel-inspired Tailoring of Membrane Wettability for Harsh Water Treatment. *J. Mater. Chem. A* **2015**, *3*, 2650−2657.
(29) Ye, Q.; Zhou, F.; Liu, W. Bioinspired Catecholic Chemistry for Surface Modification. *Chem. Soc. Rev.* **2011**, *40*, 4244−4258.
(30) Yang, H.-C.; Luo, J.-Q.; Lv, Y.; Shen, P.; Xu, Z.-K. Surface Engineering of Polymer Membranes via Mussel-inspired Chemistry. *J. Membr. Sci.* **2015**, *483*, 42−59.
(31) Della Vecchia, N. F.; Avolio, R.; Alfe, M.; Errico, M. E.; Napolitano, A.; d'Ischia, M. Building-Block Diversity in Polydopamine Underpins a Multifunctional Eumelanin-Type Platform Tunable Through a Quinone Control Point. *Adv. Funct. Mater.* **2013**, *23*, 1331−1340.
(32) Liebscher, J.; Mrowczynski, R.; Scheidt, H. A.; Filip, C.; Hadade, N. D.; Turcu, R.; Bende, A.; Beck, S. Structure of Polydopamine: A Never-ending Story? *Langmuir* **2013**, *29*, 10539−10548.
(33) Hong, S.; Na, Y. S.; Choi, S.; Song, I. T.; Kim, W. Y.; Lee, H. Non-covalent Self-Assembly and Covalent Polymerization Co-contribute to Polydopamine Formation. *Adv. Funct. Mater.* **2012**, *22*, 4711−4717.
(34) Ding, Y.; Weng, L. T.; Yang, M.; Yang, Z.; Lu, X.; Huang, N.; Leng, Y. Insights into the Aggregation/deposition and Structure of a Polydopamine Film. *Langmuir* **2014**, *30*, 12258−12269.
(35) Della Vecchia, N. F.; Avolio, R.; Alfè, M.; Errico, M. E.; Napolitano, A.; d'Ischia, M. Building-Block Diversity in Polydopamine Underpins a Multifunctional Eumelanin-Type Platform Tunable Through a Quinone Control Point. *Adv. Funct. Mater.* **2013**, *23*, 1331−1340.
(36) Bernsmann, F.; Ball, V.; Addiego, F.; Ponche, A.; Michel, M.; Gracio, J. J.; Toniazzo, V.; Ruch, D. Dopamine-melanin Film Deposition Depends on the Used Oxidant and Buffer Solution. *Langmuir* **2011**, *27*, 2819−2825.
(37) Lee, H.; Scherer, N. F.; Messersmith, P. B. Single-molecule Mechanics of Mussel Adhesion. *Proc. Natl. Acad. Sci. U.S.A.* **2006**, *103*, 12999−13003.
(38) Liu, Y.; Chang, C. P.; Sun, T. Dopamine-assisted Deposition of Dextran for Nonfouling Applications. *Langmuir* **2014**, *30*, 3118−3126.
(39) Kang, S. M.; Hwang, N. S.; Yeom, J.; Park, S. Y.; Messersmith, P. B.; Choi, I. S.; Langer, R.; Anderson, D. G.; Lee, H. One-Step Multipurpose Surface Functionalization by Adhesive Catecholamine. *Adv. Funct. Mater.* **2012**, *22*, 2949−2955.
(40) Yang, H. C.; Pi, J. K.; Liao, K. J.; Huang, H.; Wu, Q. Y.; Huang, X. J.; Xu, Z. K. Silica-Decorated Polypropylene Microfiltration Membranes with a Mussel-inspired Intermediate Layer for Oil-in-water Emulsion Separation. *ACS Appl. Mater. Interfaces* **2014**, *6*, 12566−12572.
(41) Zhang, Y.; Thingholm, B.; Goldie, K. N.; Ogaki, R.; Stadler, B. Assembly of Poly(dopamine) Films Mixed with a Nonionic Polymer. *Langmuir* **2012**, *28*, 17585−17592.
(42) Cui, J.; Ju, Y.; Liang, K.; Ejima, H.; Lorcher, S.; Gause, K. T.; Richardson, J. J.; Caruso, F. Nanoscale Engineering of Low-fouling Surfaces through Polydopamine Immobilisation of Zwitterionic Peptides. *Soft Matter* **2014**, *10*, 2656−2663.
(43) Feng, S.; Duan, L.; Hou, L.; Qiao, J.; Zhang, D.; Dong, G.; Wang, L.; Qiu, Y. A Comparison Study of the Organic Small Molecular Thin Films Prepared by Solution Process and Vacuum Deposition: Roughness, Hydrophilicity, Absorption, Photoluminescence, Density, Mobility, and Electroluminescence. *J. Phys. Chem. C* **2011**, *115*, 14278−14284.
(44) Xi, Z. Y.; Xu, Y. Y.; Zhu, L. P.; Wang, Y.; Zhu, B. K. A Facile Method of Surface Modification for Hydrophobic Polymer Membranes based on the Adhesive Behavior of Poly(DOPA) and Poly(dopamine). *J. Membr. Sci.* **2009**, *327*, 244−253.

DOI: 10.1021/acsami.5b00894
ACS Appl. Mater. Interfaces 2015, 7, 9534−9545

(45) Chen, P.-C.; Wan, L.-S.; Xu, Z.-K. Bio-inspired $CaCO_3$ Coating for Superhydrophilic Hybrid Membranes with High Water Permeability. *J. Mater. Chem.* **2012**, *22*, 22727−22733.
(46) Jiang, J.; Zhu, L.; Zhu, B.; Xu, Y. Surface Characteristics of a Self-polymerized Dopamine Coating Deposited on Hydrophobic Polymer Films. *Langmuir* **2011**, *27*, 14180−14187.
(47) Zhang, W.; Shi, Z.; Zhang, F.; Liu, X.; Jin, J.; Jiang, L. Superhydrophobic and Superoleophilic PVDF Membranes for Effective Separation of Water-in-oil Emulsions with High Flux. *Adv. Mater.* **2013**, *25*, 2071−2076.

DOI: 10.1021/acsami.5b00894
ACS Appl. Mater. Interfaces 2015, 7, 9534−9545